ORIGINAL ARTICLE

WILEY

A novel, centrally acting mammalian aminosterol, ENT-03, induces weight loss in obese and lean rodents

Denise Barbut MD[1,2] | William A. Kinney PhD[1,2] | Hsiao-Huei Chen PhD[3] |
Alexandre F. R. Stewart PhD[4] | Jacob Hecksher-Sørensen PhD[5] |
Chen Zhang PhD[6] | Alexander Fleming MD[7] | Michael Zemel PhD[7] |
Michael Zasloff MD, PhD[1,2,8]

[1]Enterin, Inc., Philadelphia, Pennsylvania, USA

[2]Enterin Research Institute, Philadelphia, Pennsylvania, USA

[3]Ottawa Hospital Research Institute, Ottawa, Ontario, USA

[4]University of Ottawa Heart Institute, Ottawa, Ontario, USA

[5]Gubra, Aps, Copenhagen, Denmark

[6]Novo Nordisk, Copenhagen, Denmark

[7]Kinexum, Harpers Ferry, West Virginia, USA

[8]MedStar Georgetown Transplant Institute, Washington, District of Columbia, USA

Correspondence
Michael Zasloff, MedStar Georgetown Transplant Institute, Georgetown University Hospital, 2 PWC 3800 Reservoir Road, NW Washington, D.C. 20007, USA.
Email: maz5@georgetown.edu

Funding information
Canadian Institutes of Health Research, Grant/Award Numbers: 376403, 376503; Weston Brain Institute of the Weston Family Foundation, Grant/Award Number: TR-10083; Natural Sciences and Engineering Research Council of Canada, Grant/Award Numbers: RGPIN-2019-03942, RGPIN-2016-04985

Abstract

ENT-03, a spermine bile acid we recently discovered in the brain of newborn mice acts centrally to regulate energy and metabolism. Obese, diabetic (ob/ob) mice treated with five doses of ENT-03 over 2 weeks, demonstrated a rapid decrease in blood glucose levels into the range seen in non-obese animals, prior to any significant weight loss. Weight fell substantially thereafter as food intake decreased, and serum biochemical parameters normalized compared with both vehicle and pair-fed controls. To determine whether ENT-03 could be acting centrally, we injected a single dose of ENT-03 intracerebroventricularly to Sprague–Dawley rats. Weight fell significantly and remained below vehicle injected controls for an extended period. By autoradiography, ENT-03 localized to the arcuate nucleus of the hypothalamus, the choroid plexus and cerebrospinal fluid. Significant cFos activation occurred in multiple anatomical regions within the hypothalamus and brainstem involved in appetite suppression, food-entrained circadian rhythmicity, autonomic function, and growth. These data support a role for ENT-03 in the treatment of type 2 diabetes and obesity. Phase 1 studies in subjects with obesity and diabetes are currently in progress.

KEYWORDS
aminosterol, obesity, PTP1B inhibitor, trodusquemine, type 2 diabetes

1 | INTRODUCTION

Trodusquemine (MSI-1436; Figure 1) was discovered during the isolation and characterization of novel amino steroids present in the liver of the dogfish shark.[1] It was subsequently demonstrated that trodusquemine induces profound metabolic effects in several vertebrate species, including humans. When administered to obese mice, trodusquemine reduced food intake, adiposity and body weight,[2,3] increased insulin sensitivity and reversed fatty liver disease.[4] Subsequently, the compound was shown to inhibit PTP1B, providing a mechanism for its pharmacology in several in vivo studies.[5–8] In early-stage human clinical trials, it exhibited dose-dependent weight reduction and increased insulin sensitivity.[9]

We hypothesized that an orthologue of the shark molecule would be present in mammals. Since the bile alcohols of the shark and lamprey are replaced by bile acids in mammals,[10] we considered it likely
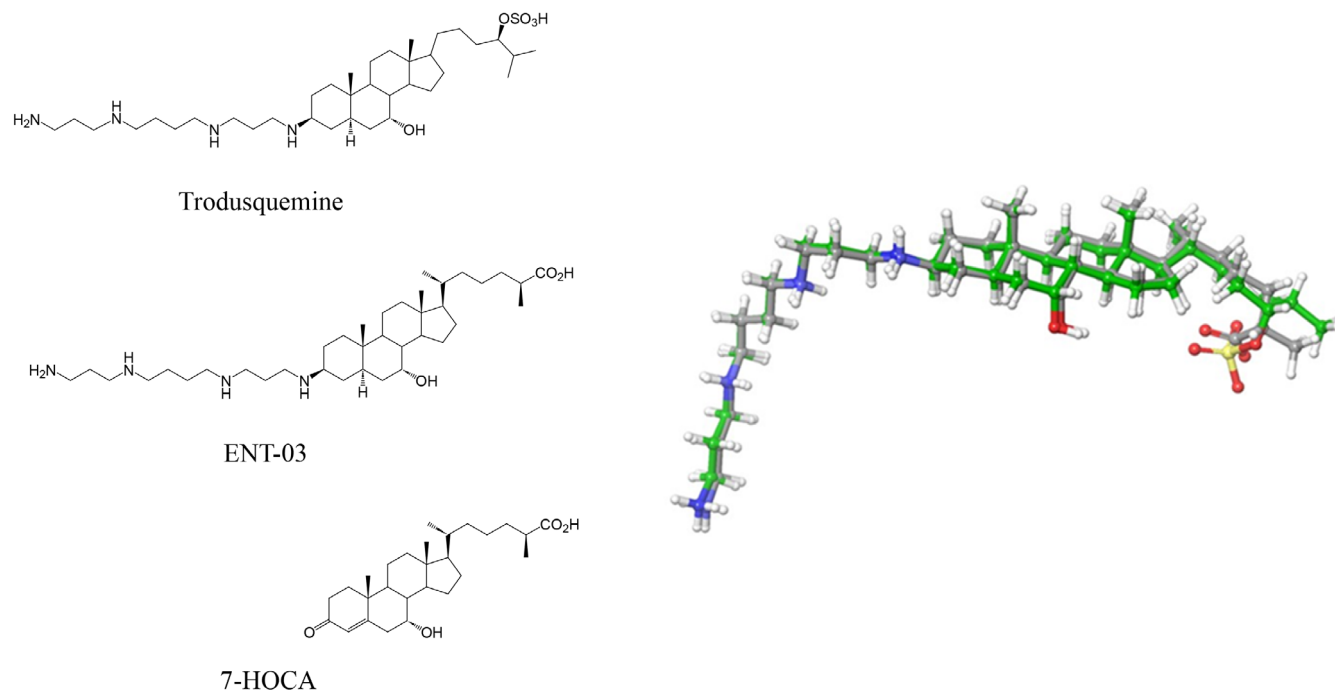
FIGURE 1 Shark trodusquemine, mammalian ENT-03 and mammalian 7-alpha-hydroxy-3-oxo-4-cholestenoic acid. The three-dimensional structures of trodusquemine (green) and ENT-03 (grey) are overlapped.

that the steroidal moiety of a mammalian analogue of the shark molecule would be represented by a C-27 planar bile acid rather than a sulphate ester. C-27 bile acids, such as 7-alpha-hydroxy-3-oxo-4 cholestenoic acid (7-HOCA; Figure 1), are among the most abundant bile acids present in mouse and human cerebrospinal fluid (CSF).[11,12] In humans, 7-HOCA is synthesized in the brain and secreted into the systemic circulation.[13] Conceptually, the coupling of spermine to 7-HOCA, followed by reductions at C3 and C5 of the steroid, would yield the proposed compound. We subsequently identified a candidate molecule in the tissues of the neonatal mouse, which we named ENT-03 (Figure 1). The discovery and chemical synthesis of this compound is described elsewhere.[14]

In this report, we describe the pharmacological properties of ENT-03 in normal and obese diabetic rodents. We show that ENT-03 appears to exert its metabolic effects by action on the brain and describe, through whole-brain cFos mapping and autoradiography, the probable sites of action. Phase 1 clinical trials evaluating the safety, tolerability, pharmacokinetics, and signals of efficacy in obese subjects with and without type 2 diabetes have been initiated (NCT05925920).

2 | METHODS

2.1 | Aminosteroids

The synthesis of ENT-03 is described in detail elsewhere.[14] The compound used was more than 98% pure. Mouse and rat experiments are described in detail in Data S1.

2.2 | Whole-brain mapping

The whole-brain mapping studies were performed by Gubra Aps and the methods are described in detail in Data S1.

2.3 | Quantitative whole-brain autoradiography

The quantitative whole-brain autoradiography studies were conducted at Pharmaron UK, and the methods are described in Data S1.

2.4 | Statistics

Statistical analyses were conducted with the level of significance set at $p < 0.05$. The group means, standard deviation, standard error of the mean, and t-tests were calculated for specific experiments, as noted. One-way analysis of variance comparisons among the groups were performed with GraphPad Prism 8.0 software.

3 | RESULTS

3.1 | Effects of ENT-03 on diabetic, obese *ob/ob* mice

ENT-03 was administered to 4-month-old *ob/ob* mice (male, 45 g) 10 mg/kg every 3 days by intraperitoneal (i.p.) injection for a total of five doses (13 days). A vehicle-treated cohort was included that

received the same amount of food consumed by the ENT-03-treated animals ('pair-fed') to identify effects of ENT-03 that occurred beyond reduced food intake. Mice were fed standard laboratory chow.

One day after the initial dose of ENT-03 was administered, mean fasting blood glucose levels (6.4 ± 1.0 mmol/L) of the treated mice was within the normal range, 46% lower than vehicle-treated mice (10.7 ± 1.0 mmol/L; $p < 0.01$), and 50% lower than the pair-fed mice (12.2 ± 1.5 mmol/L; $p < 0.01$ [Figure 2]). Over the duration of the treatment period, the body weight of the treated mice fell by approximately 6%, while that of the pair-fed cohort fell by approximately 8%. These data demonstrate that a single administration of ENT-03 can acutely normalize blood glucose in obese diabetic mice before weight loss can be detected.
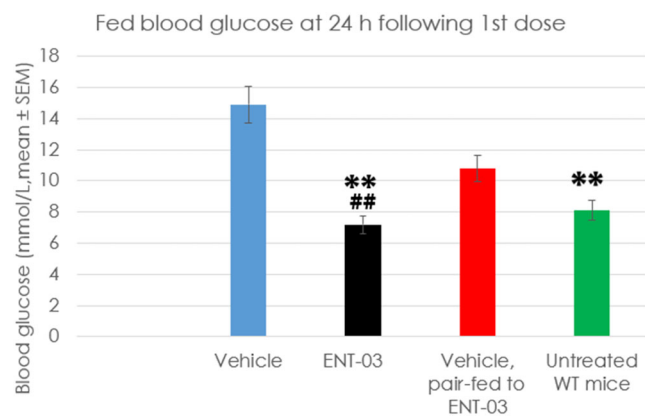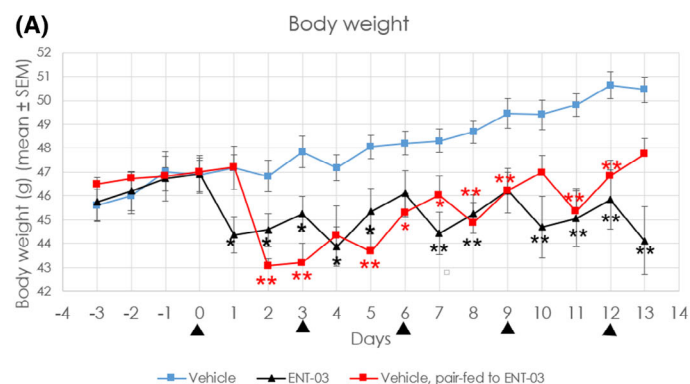

FIGURE 2 Effect of a single dose of ENT-03 on blood glucose. Fasting blood glucose was measured 24 h following the first administration of ENT-03 or vehicle ($N = 4$/group). **$p < 0.01$ compared with the vehicle group by one-way analysis of variance; ##$p < 0.01$ compared ENT-03 group with the pair-fed group by t-test.

Over the 13 days of the study, the cumulative food consumed by the ENT-03-treated mice was 20% lower at Day 13 than that consumed by vehicle-treated mice ($p < 0.01$), which was matched by the vehicle-treated pair-fed group (Figure 3). The vehicle-treated mice increased body weight by approximately 11%, the ENT-03 group lost approximately 4% of body weight from the start of the study, while the pair-fed mice maintained their starting weight (Figure 3). However, the ENT-03-treated mice lost significantly more body fat compared with the vehicle group (13.7%; $p < 0.05$), while the loss of body fat between the pair-fed cohort and the vehicle group was not statistically different (4%; p = nonsignificant) as measured by X-ray densitometry (Faxitron® DXA digital radiography system [Table 1]).

On Day 13, after five doses of ENT-03, the non-fasting blood glucose of the ENT-03-treated group (7.2 mM) was reduced by approximately 50% compared to the blood glucose in the vehicle group (14.9 mM), and was not different from that of wild-type (WT) mice (8.1 mM), while the pair-fed group showed a less marked correction (10.8 mM; Table 2). Serum insulin levels were elevated at 26.5 ng/mL in vehicle-treated mice and 34.7 ng/mL in pair-fed mice compared to 13.8 ng/mL in ENT-03-treated mice ($p < 0.01$). Serum total ghrelin concentrations, elevated in *ob/ob* mice, were markedly reduced to near-normal concentrations by ENT-03 treatment but unchanged by food restriction. Serum growth hormone concentrations in *ob/ob* mice were low compared to the WT mice.[15,16] ENT-03 treatment increased growth hormone concentration by approximately 75% compared to the vehicle group, while pair-feeding had no impact. These data demonstrate that ENT-03 treatment increased insulin sensitivity and normalized both ghrelin and growth hormone, and that these effects cannot be solely attributed to food restriction and the ensuing weight loss.

Total triglycerides, total cholesterol and total ketones did not differ significantly among the three groups.

The liver weight of the ENT-03-treated mice was significantly reduced (35%; $p < 0.01$) by a greater magnitude than the pair-fed
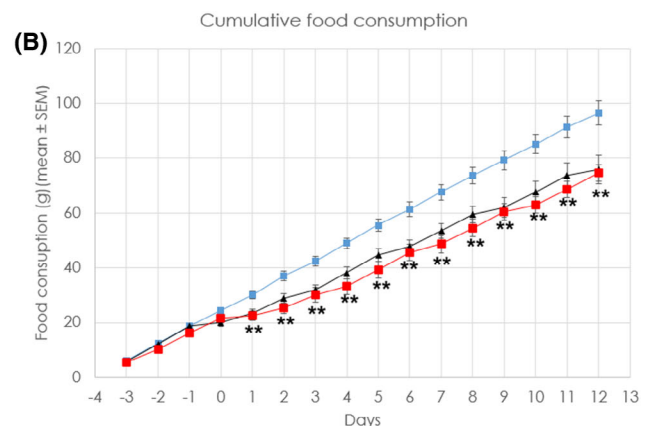
FIGURE 3 Effect of ENT-03 on body weight and food intake in *ob/ob* mice ($n = 4$) in all cohorts. Blue squares, vehicle. Red squares, vehicle-treated, but pair-fed to ENT-03 cohort. Black triangles, ENT-03 treatments. (A) Body weight: vehicle versus ENT-03, $p < 0.01$; vehicle versus pair-fed, $p < 0.05$ (one-way ANOVA). (B) Cumulative food consumption: vehicle versus ENT-03, $p < 0.01$ (one-way analysis of variance [ANOVA]). *$p < 0.5$; **$p < 0.01$, treated and pair-fed versus vehicle (t-test). Dosing days noted along the horizontal axis. Data are means ± standard error.

(15%; $p < 0.05$) compared with the vehicle group (Figure 4). Liver tissues of the vehicle group were characterized by micro- and macro-vesicular steatosis, prominent in the pericentral region, with relative sparing of the portal areas (Figure 4). Severity of the steatosis was markedly reduced in the ENT-03 group and to a lesser degree in the pair-fed mice. Serum alanine aminotransferase, a measure of liver injury, was markedly lower in the ENT-03-treated cohort compared with the vehicle group (704 U/L vs. 173 U/L; $p < 0.001$), consistent with an improvement in hepatic steatosis, while the pair-fed animals exhibited a more modest reduction (704 U/L vs. 384 U/L; $p =$ nonsignificant [Table 2]). These observations suggest that ENT-03 preferentially mobilized lipid from the liver and adipose tissue, and that these effects are greater than can be explained solely by weight loss and food restriction.

3.2 | Effects on metabolism in ad libitum-fed WT mice following chronic administration

To address the effects of ENT-03 on energy metabolism following chronic dosing, male C57bl/6j mice were dosed intranasally (2 mg/kg/3.5 days) over 2.5 months. The intranasal route was chosen for ease of administration over a prolonged period. Dosing was adjusted such that the treated mice maintained a stable body weight of approximately 90% of vehicle-treated animals (Figure S1A). The animals were then transferred to metabolic chambers immediately following an intranasal administration of either ENT-03 or vehicle. The respiratory exchange ratio of the ENT-03 group fell to approximately 0.8 during daylight hours compared to approximately 0.9 for the vehicle-treated cohort, indicating increased lipid catabolism (Figure S1B1,B2). This was associated with a decrease in food intake (Figure S1C) and body weight (Figure S1D0). Body temperature (Figure S1E1–E3) and locomotor activity (Figure S1F1–G3) were not affected.

The cohorts were then returned to standard cages, administered either ENT-03 or vehicle for two successive doses (2 mg/kg/3.5 days). One hour after the last intranasal administration of either ENT-03 or vehicle, the animals were administered a glucose tolerance test (i.p.), which demonstrated that ENT-03 treatment had improved glucose tolerance in these lean mice ($p < 0.05$ [Figure S1H]).

3.3 | ENT-03 acts centrally

Male rats fed ad libitum on a standard chow diet were administered ENT-03 via an intracerebroventricular cannula in a single dose of 60 or 120 μg per animal (∼0.17 mg/kg and 0.34 mg/kg, respectively [Figure 5]). When administered systemically these doses of ENT-03 have no measurable pharmacological effect. ENT-03 administered centrally caused a dose-dependent decrease in body weight over the first few days after injection, associated with a decrease in food intake followed by resumption of weight gain on a new parallel. Treated rats maintained reduced body weight and reduced food intake relative to the untreated cohorts for at least 2 weeks.

3.4 | Localization of ENT-03 within the brain following systemic administration

To determine the locations within the brain to which ENT-03 directly binds, a single dose of ^{3}H-ENT-03 (1 mg/kg) was administered

TABLE 1 Body composition of *ob/ob* mice determined by X-ray densitometry.

Treatment	Body composition	
	Lean tissue, g	Adipose tissue
Vehicle	25.0 ± 1.3	25.4 ± 2.4
ENT-03	22.5 ± 1.2*	21.9 ± 2.3*
Pair-fed	22.9 ± 0.7	24.4 ± 1.9
Untreated WT mice	22.0 ± 1.2	2.8 ± 0.2**

Note: *$p < 0.05$, **$p < 0.01$ compared with the vehicle group by one-way analysis of variance. Lean tissue estimates include both muscle and liver. Data are expressed as means ± standard error.
Abbreviation: WT, wild-type.

TABLE 2 Serum biochemical parameters associated with the *ob/ob* study.

Biochemical parameter	Vehicle	ENT-03	Pair-fed	WT, untreated
Serum glucose, mM	14.9 ± 1.1	**7.2 ± 1.9****	10.8 ± 3.4*	8.1 ± 0.4**
Serum insulin, ng/mL	26.5 ± 8.1	**13.8 ± 5.6**##**	34.7 ± 40.1	1.2 ± 0.3 **
Serum ghrelin, ng/mL	14.5 ± 4.8	**8.2 ± 0.8*##**	17.5 ± 3.1	5.2 ± 1.9**
Serum growth hormone, ng/mL	0.42 ± 0.26	**0.79 ± 0.19#**	0.32 ± 0.14	0.56 ± 0.06
Leptin, pg/mL	181 ± 7	143 ± 15	121 ± 12	1388. ± 3**
ALT, U/L	704 ± 193	**173 ± 106****	384 ± 258	53 ± 10**
Total triglycerides, mM	1.84 ± 0.10	1.80 ± 0.24	1.26 ± 0.14	1.35 ± 0.41
Total cholesterol, mM	5.2 ± 0.5	5.6 ± 0.5	4.9 ± 0.5	2.3 ± 0.4**
Ketones, mM	0.59 ± 0.4	0.52 ± 0.5	1.7 ± 2.9	0.72 ± 0.4

Note: Blood samples were obtained 1 day after the final ENT-03 dose administered. Means ±SD values are shown. *$p < 0.05$, **$p < 0.01$ compared with the vehicle group by one-way analysis of variance. #$p < 0.05$, ##$p < 0.01$ compared ENT-03 with pair-fed by *t*-test.
Abbreviations: ALT, alanine aminotransferase; WT, wild-type.

(A)

Treatment	Tissue weight (g)
	Liver
Vehicle	3.70 ± 0.14
ENT-03S	2.42 ± 0.37**
Pair-fed	3.14 ± 0.28*
Untreated WT mice	1.12 ± 0.13***

(B)
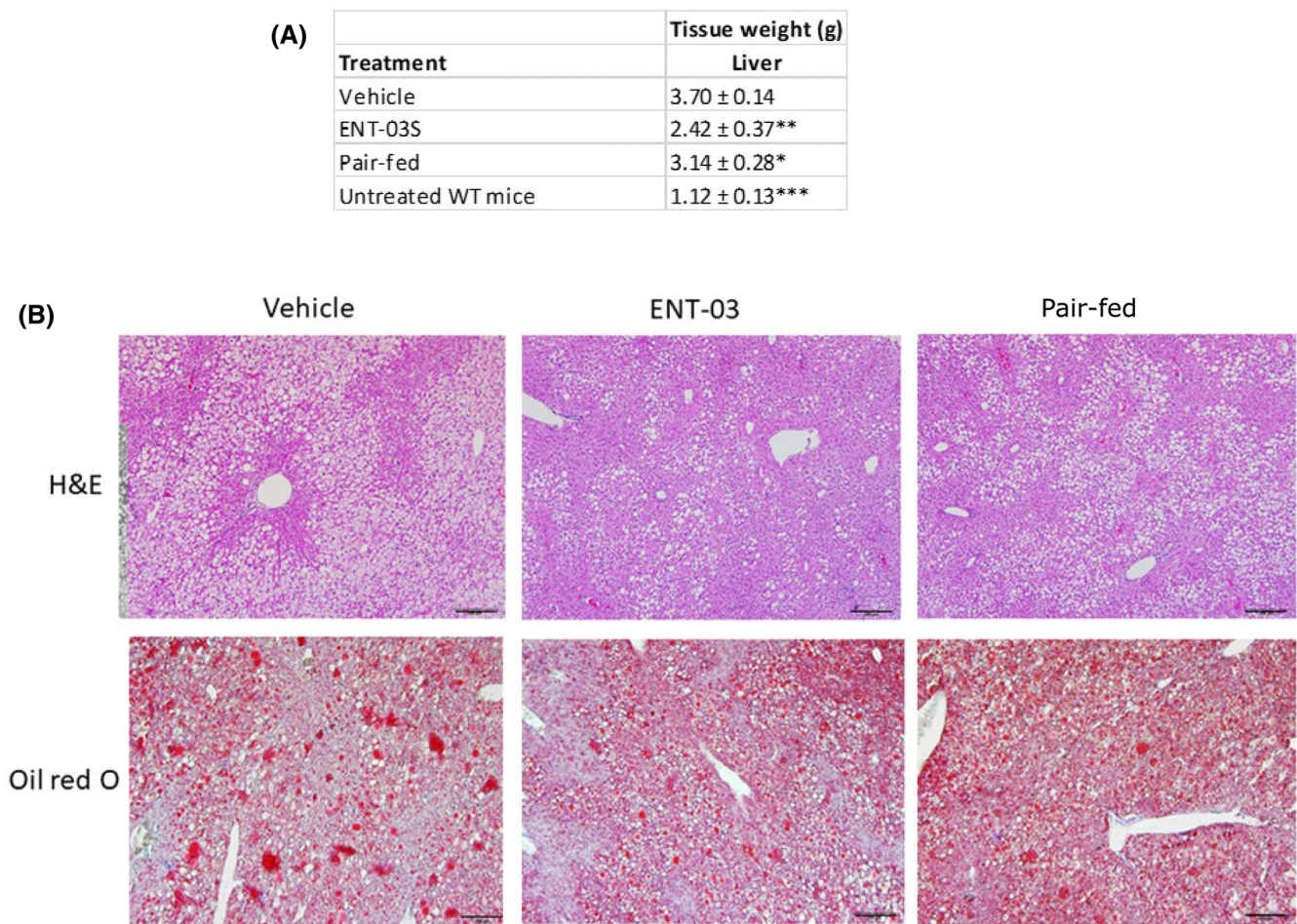
FIGURE 4   ENT-03 reduces hepatic steatosis. (A) Mean liver weight post necropsy. $*p < 0.5$; $**p < 0.01$, experimental groups versus vehicle, by t-test; $***p < 0.001$, wild-type (WT) versus ob/ob, both untreated. (B) Representative micrographs. Top row: hematoxylin and eosin (H&E)-stained tissue; bottom row: oil red O-stained. Left column: vehicle; middle column, ENT-03-treated; right column: vehicle treated, pair-fed to ENT-03 cohort ($100\times$; 200 μm bar).
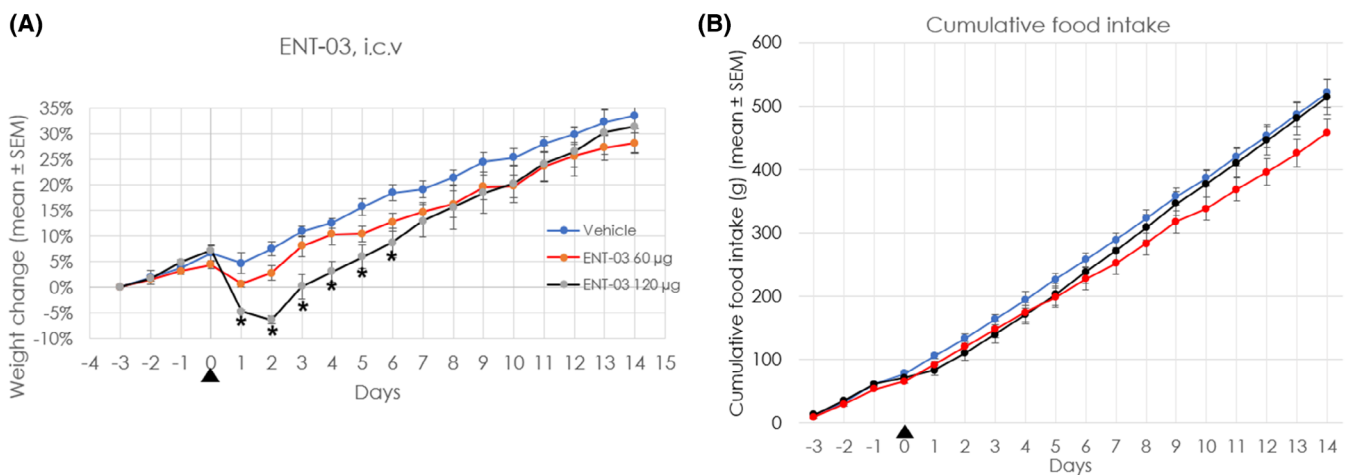
FIGURE 5   Effect of intracerebroventricular (i.c.v.) administration of a single dose of ENT-03 on weight gain and food intake in lean rats. (A) Weight. (B) Food intake. ENT-03, or vehicle, was administered i.c.v. on Day 0 to male SD rats (200–250 g, $N = 3$–4/group) at 60 μg and 120 μg. $*p < 0.05$; $**p < 0.01$, vehicle versus treated animals (t-test). Data are means ±standard error.
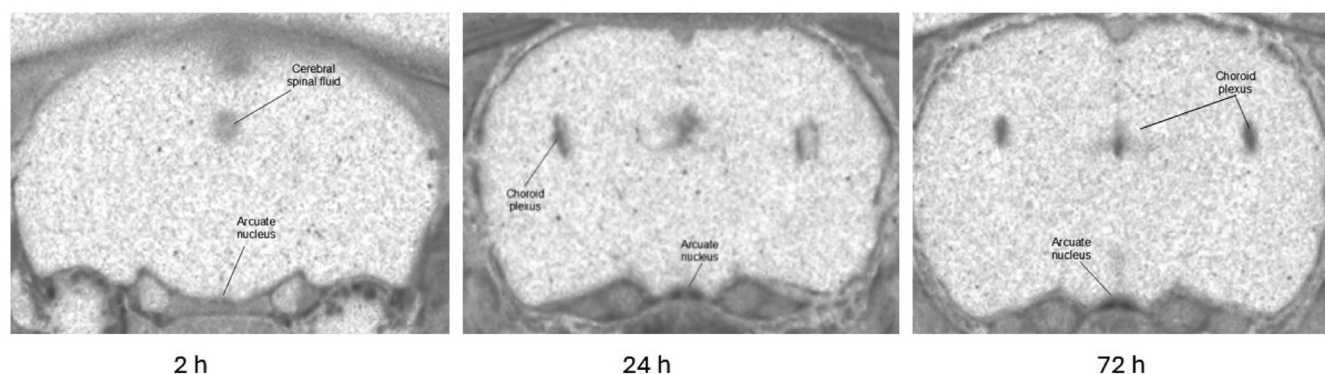
FIGURE 6 Autoradiographic localization of systemically administered ^{3}H-ENT-03. Individual rats were euthanized at noted times after dosing. Coronal sections through the arcuate nucleus are shown. The choroid plexus within the third and lateral ventricles appears at 24 h.

TABLE 3 Distribution of ^{3}H-ENT-03 in rat brain and cardiac blood by quantitative autoradiography.

	2 h	6 h	24 h	72 h
Arcuate nucleus	**0.538**	**0.789**	**2.20**	**3.37**
Brain whole	BLQ	0.012	BLQ	BLQ
Brain olfactory bulb	BLQ	BLQ	0.014	BLQ
Brain cerebral cortex	BLQ	0.035	BLQ	BLQ
Brain cerebellum	BLQ	0.021	BLQ	0.013
Brain hypothalamus	BLQ	0.016	BLQ	BLQ
Choroid plexus	**0.382**	**0.529**	**0.907**	**1.95**
Cerebrospinal fluid	**0.153**	**0.116**	**0.118**	**0.133**
Cardiac blood	9.40	4.60	2.99	0.67

Note: Concentration values are expressed in terms of μg equivalents of test compound/g tissue. The lower limit of quantification was 0.009 μg equivalents/g. Tissues containing visible radioactivity below this limit are designated 'BLQ' (below limit of accurate quantification).

intravenously to ad libitum-fed male Sprague–Dawley rats. The brain was perfused with saline prior to euthanasia at 2, 6, 24 and 72 h to clear radioactivity within the blood stream from the tissues. The distribution of radioactivity within the brain was determined by autoradiography of brain slices. Appreciable amounts of ENT-03 in the brain were limited to the region encompassing the arcuate nucleus of the hypothalamus, the choroid plexus and the CSF (Figure 6 and Table 3). Although blood levels of ENT-03 fell over the course of the 72-h study (Table 3), concentrations of ENT-03 increased progressively within the arcuate nucleus and the choroid plexus. By 72 h, the highest concentration of ENT-03 was localized to the arcuate nucleus.

3.5 | ENT-03 inhibits PTP1b and induces phosphorylation of STAT3 in the hypothalamus and choroid plexus

Trodusquemine inhibits human protein tyrosine phosphatase PTP1B by binding to two allosteric sites.[5] ENT-03 was assayed for PTP1B inhibitory activity using either intact F11 neuronal cells or whole cell lysates (Data S1). The observed concentration required to inhibit PTP1B by 50% for ENT-03 against PTP1B assayed with intact cells was approximately 1×10^{-8} M, and approximately 5×10^{-7} M when assayed against cellular lysates, similar to the activity of trodusquemine (Figure S2).

PTP1B is known to downregulate the activity of both the insulin and leptin signalling pathways.[17] Inhibition of PTP1B activity, as a consequence, increases insulin and leptin signalling. PTP1B depresses insulin signalling by the dephosphorylation of the activated insulin receptor as well as downstream targets.[18] To determine whether ENT-03 could alter insulin signalling, serum-starved F11 neuronal cells were exposed to vehicle or ENT-03 (10 or 100 nM) for 30 min, followed by a 5-min incubation in the presence or absence of insulin. ENT-03 treatment increased the relative abundance of the insulin-dependent phosphorylated receptor (pIRb/IRb) more than threefold at both concentrations of ENT-03 (Figure S2). Interestingly, significant ENT-03-dependent phosphorylation of the insulin receptor was also observed in the absence of exogenous insulin.

Since ENT-03 can inhibit PTP1B in the context of intact neuronal cells, we investigated whether the presence of ENT-03 within the arcuate nucleus and the choroid plexus exhibited the anticipated action with respect to either the PI3K-AKT or JAK–STAT3 pathways within these sites. We initially visualized effects on these pathways within the whole brain to avoid missing areas not captured by the autoradiographic procedure. Mice received a dose of ENT-03 (10 mg/kg) by i.p. administration and were euthanized 2 h later. We examined the distribution of both phosphorylated AKT (pAKT) and STAT3 (pSTAT3) by immunofluorescence of the intact mouse brain, visualizing the localization of antibody with light sheet microscopy and three-dimensional reconstruction.

Of the two target proteins, pSTAT3 demonstrated the most robust signal (Figure 7A and Movie S1). The choroid plexus was the most intensely stained of the brain structures at this time point, suggesting that JAK–STAT3 signalling pathways within the choroid plexus are responsive to ENT-03. Furthermore, ENT-03 that accesses the choroid plexus appears to be secreted into the CSF, based on the autoradiographic study. A few scattered pSTAT3+ neurons within the arcuate could be identified (Movie S1, pSTAT3).
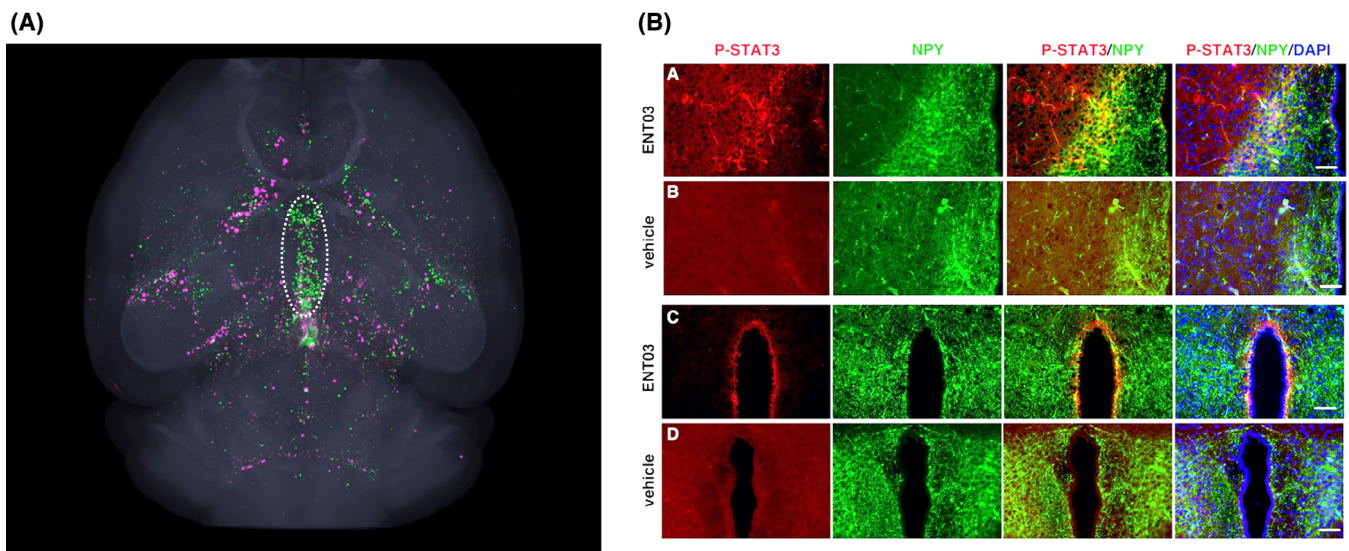
FIGURE 7 Distribution of immune-stained phosphorylated STAT3 (pSTAT3) following systemic administration of ENT-03. (A) Whole-brain three-dimensional reconstruction of pSTAT3 staining. Mice were euthanized 2 h following intraperitoneal administration of either vehicle or ENT-03 (10 mg/kg; N = 2/cohort), and the brain subsequently processed as described in the Methods. The signals from the vehicle-treated mice are imaged in magenta, the signals from the ENT-03-treated mice, in green. The data from all four animals have been superimposed to create the composite image. The choroid plexus within the third ventricle is highlighted. See Movie S1 for a more detailed view. (B) Mice were treated with either vehicle or ENT-03 for 3 weeks and the brains immune-stained for pSTAT3. Sections through (A, B) arcuate nucleus and (C, D) subventricular zone (SVZ) at the third ventricle from mice treated with ENT-03 (A, C) or vehicle (B, D) were stained for pSTAT3 (in red) and neuropeptide Y (NPY; in green) and nuclei were counterstained with DAPI. Scale bar, 50 μm.

We next explored the effect of a longer period of ENT-03 dosing on the pSTAT3 signal within the medial basal hypothalamus. Male C57bl/6j mice fed normal laboratory chow were administered ENT-03 by the i.p. route (10 mg/kg, twice weekly, for 3 weeks). The hypothalamic tissues were then immune-stained for pSTAT3 to identify cells in which JAK-STAT pathways were activated. Neuropeptide Y (NPY) was also visualized to identify the arcuate nucleus. The pSTAT3 signal within the arcuate nucleus was markedly increased in ENT-03-treated animals compared with controls (Figure 9; lower panel). Its localization lateral to the cluster of NPY-expressing cells, places the pSTAT3 signal within the region containing neurons with the highest concentration of leptin receptors.[19,20] We also observed an intense pSTAT3 signal within cells located within the subventricular zone of the third ventricle (Figure 7B), compared with untreated animals, possibly a result of stimulation by ENT-03 present in the CSF.

3.6 | ENT-03 upregulates cFos activation in brain regions involved in satiety and appetite regulation

Three-dimensional cFos imaging was utilized to obtain a whole brain view of the neurons activated following systemic administration of ENT-03. The expression of cFos, a transcription factor, is induced rapidly in neurons following a stimulus and thus serves as a widely used marker for neuronal activation and activity. Lean C57bl/6jR mice received a single i.p. injection of vehicle or ENT-03 and were euthanized 2 h later. Isolated brains were stained for cFos and imaged at single-cell resolution using light sheet microscopy. cFos data from individual brains were mapped onto an average mouse brain atlas template and the number of cFos-labelled cells was quantified in 286 brain regions, using previously described methods.[21] Olfactory bulbs were not analysed.

Over 40 anatomical sites were stimulated at high significance (p < 0.001; see Data S1) in comparison to the vehicle-treated animals (Figures 8 and 9, Movie S2 cFos). An acute parenteral dose of ENT-03 led to strong cFos activation in multiple hypothalamic areas involved in appetite suppression, food entrained circadian rhythmicity, autonomic function, and growth: the proopiomelanocortin region of the arcuate nucleus, the tuberal nucleus, the parastrial nucleus, the lateral preoptic nucleus, the dorsomedial nucleus, the ventral premammillary nuclei, and the paraventricular nucleus and its periventricular area (paraventricular hypothalamic nucleus [PVH]; Figure 9 and Movie S2, cFos). ENT-03 also activated multiple brainstem nuclei, which enable responses to stress, such as the level of alertness (various reticular nuclei), posture (red nuclei), muscle tone (caudal pontine reticular nuclei), processing of delayed reward (dorsal raphe nucleus), locomotor activity (periaqueductal grey), midbrain reticular nucleus, pedunculopontine nuclei, inhibition of pain (nucleus raphe magnus), control of respiration, (parapyramidal nuclei), sympathetic activation (locus coeruleus), and visceral autonomic responses (Barrington's nucleus, nucleus ambiguous, nucleus tractus solitarius, the dorsal motor nucleus of the vagus, the area postrema, the parabrachial nucleus, and the parasubthalamic nucleus).
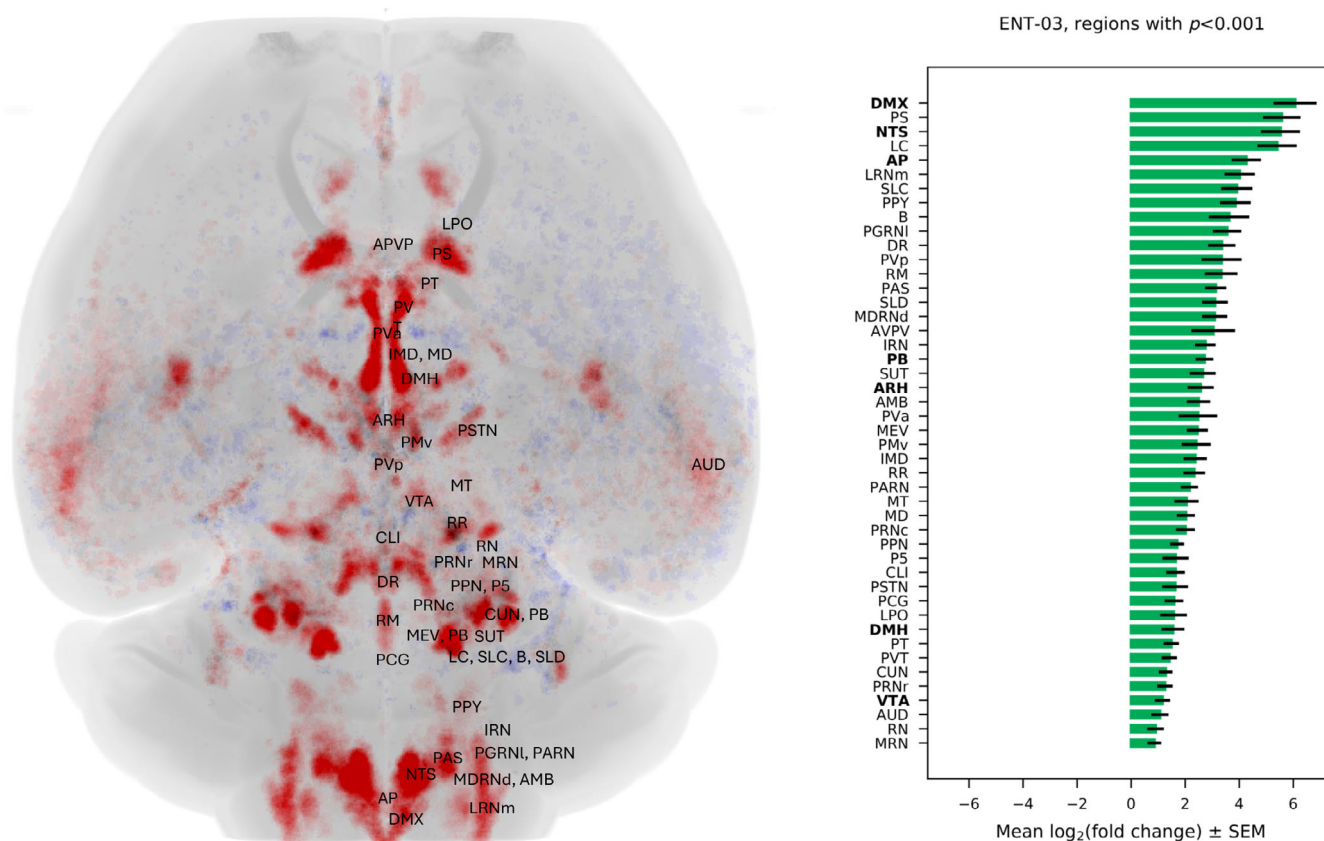
FIGURE 8 Whole-brain cFos activation map following ENT-03 administration. Left, cFos heat map (vehicle subtracted) determined 2 h following 10 mg/kg (intraperitoneal), with brain regions annotated. Right, fold increase of cFos-positive neurons above vehicle ($n = 8$ mice per treatment group). Only regions with $p < 0.001$ are presented. AMB, nucleus ambiguous; AP, area postrema; ARH, arcuate hypothalamic nucleus; AUD, auditory areas; AVPV, anteroventral periventricular nucleus; B, Barrington's nucleus; CLI, central linear nucleus raphe; CUN, cuneiform nucleus; DMH, dorsomedial hypothalamic nucleus; DMX, dorsal motor nucleus of the vagus nerve; DR, dorsal nucleus raphe; IMD, intermediodorsal nucleus of the thalamus; IRN, intermediate reticular nucleus; LC, locus coeruleus; LPO, lateral preoptic area; LRNm, lateral reticular nucleus, magnocellular part; MD, mediodorsal nucleus of thalamus; MDRNd, medullary reticular nucleus, dorsal part; MEV, midbrain trigeminal nucleus; MRN, midbrain reticular nucleus; MT, medial terminal nucleus of the accessory optic tract; NTS, nucleus of the solitary tract; P5, peritrigeminal zone; PARN, parvicellular reticular nucleus; PAS, parasolitary nucleus; PB, parabrachial nucleus; PCG, pontine central grey; PGRNl, paragigantocellular reticular nucleus, lateral part; PMv, ventral premammillary nucleus; PPN, pedunculopontine nucleus; PPY, parapyramidal nucleus; PRNc, pontine reticular nucleus, caudal part; PRNr, pontine reticular nucleus; PS, parastrial nucleus; PSTN, parasubthalamic nucleus; PT, parataenial nucleus; PVH, paraventricular hypothalamic nucleus; PVa, periventricular hypothalamic nucleus, anterior part; PVp, periventricular hypothalamic nucleus, posterior part; PVpo, periventricular hypothalamic nucleus, preoptic part; PVT, paraventricular thalamic nucleus; RN, red nucleus; RR, midbrain reticular nucleus, retrorubral area; RM, nucleus raphe magnus; SLC, subceruleus nucleus; SLD, sublaterodorsal nucleus; SUT, supratrigeminal nucleus; VTA, ventral tegmental area.

4 | DISCUSSION

The results of studies conducted with ENT-03 demonstrate that this molecule reduces food intake and body weight in the mouse and rat, with the anticipated metabolic consequences. In obese, leptin-deficient diabetic mice, ENT-03 acutely (within 24 h) normalized fasting blood glucose prior to significant weight loss. This pharmacological property of ENT-03 is also observed in diabetic, diet-induced obese mice.[22] Abnormal metabolic parameters characteristic of the *ob/ob* mouse model, such as non-fasting hyperglycaemia, fatty liver, abnormal liver function, elevated insulin and ghrelin, diminished growth

hormone, excessive food intake and weight gain were either normalized or significantly improved over the course of 2 weeks' exposure to ENT-03. The data also demonstrate that the metabolic consequences of ENT-03 administration do not result solely from reduced food intake or weight loss. *Ob/ob* mice receiving ENT-03 achieved normoglycaemia and mobilized more lipid from adipose tissue and liver than untreated cohorts that were fed the same amount of food as that consumed by the ENT-03-treated mice.

The reduction in plasma ghrelin concentrations observed in the ENT-03-treated mice is similar to the response observed in rodents and humans after bariatric surgery.[23] Procedures such as Roux-en-Y

FIGURE 9 cFos heat maps of hypothalamic regions of ENT-03 treated mice. Vehicle subtracted cFos heat maps of the ENT-03 mice of coronal sections through the hypothalamus. DMH, dorsomedial hypothalamic nucleus; ARH, arcuate hypothalamic nucleus; LPO, lateral preoptic area; PMV, ventral premammillary nucleus; PVH, paraventricular hypothalamic nucleus; PVp, periventricular hypothalamic nucleus; PVpo, periventricular hypothalamic nucleus, preoptic part; TU, tuberal nucleus.
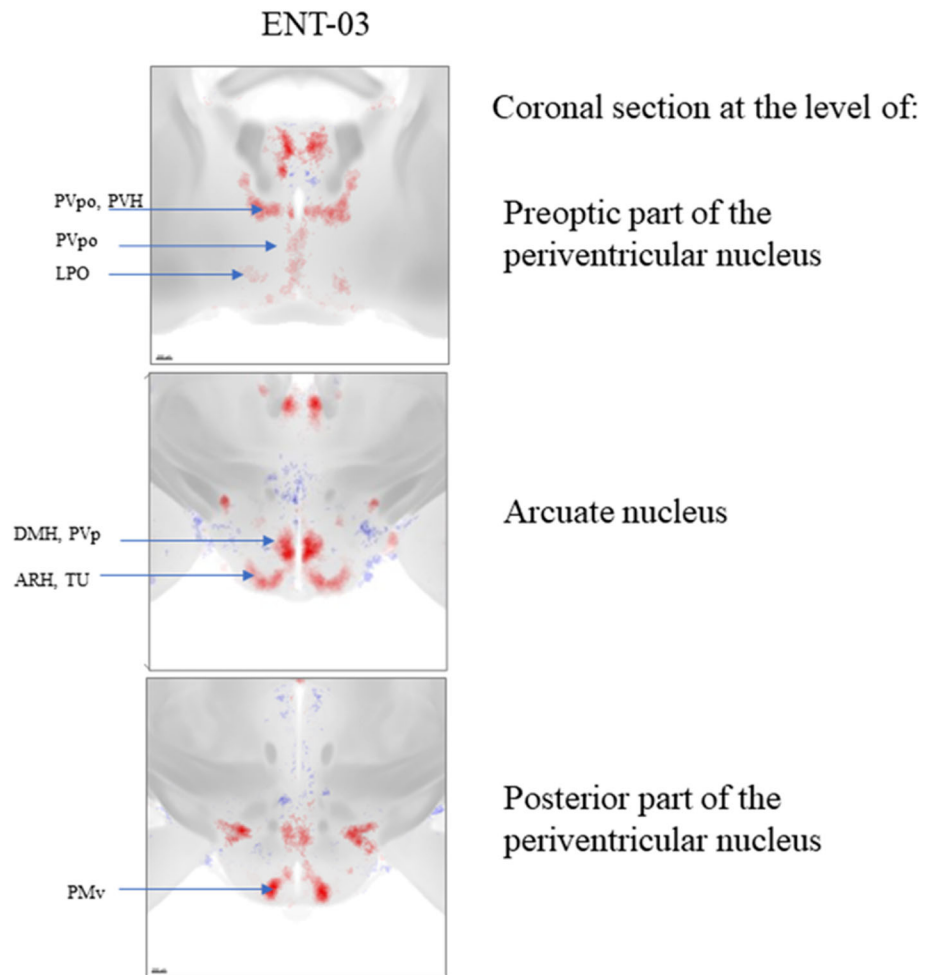
gastric bypass, gastric sleeve surgery, and ileal bile duct diversion[24] all increase circulating bile acid levels, leading to the speculation that the metabolic benefits that accrue from these procedures might involve their impact on bile acids.[24] It is possible that alteration in bile acid metabolism effected by bariatric surgery influences the levels of endogenous ENT-03, itself a product of the bile acid pathway.

Treatment of lean mice with ENT-03 over a 2-month period reduced glycaemic excursion following a glucose challenge, reduced body weight, and increased lipid catabolism, as measured by respiratory gas exchange, without affecting either the magnitude or circadian rhythm of locomotor activity or body temperature.

Since intracerebroventricular administration of ENT-03 to the lean rat resulted in reduced food intake and loss of body weight at doses far below what is required to achieve a comparable effect by systemic administration, the brain is the apparent site of action. This effect could result from either the release of hormones directed by the brain, the activation of neural pathways between the brain and liver/muscle, or both pathways. Considerable data, however, suggest a role for direct neural regulation of metabolic homeostasis.[25] For example, ENT-03 shares certain pharmacological properties with leptin. Leptin, like ENT-03, acutely corrects hyperglycaemia in leptin-deficient *ob/ob* mice following central administration.[26] Leptin

achieves this effect by enhancing the hypothalamic response to insulin,[26] which in turn, improves peripheral insulin sensitivity through autonomic neural transmission.[27]

Where in the brain is ENT-03 acting? By administering ³H-ENT-03 systemically and determining sites of localization of the compound within the brain, we have established that ENT-03 accumulates in the microanatomical region of the arcuate nucleus and the choroid plexus. (The low spatial resolution of the macroscopic autoradiographic method limited the distinguishable sites of ENT-03 to dense collections of cells, so it is possible that its presence in smaller collections of cells were not visualized.) Since tissue concentrations in the arcuate nucleus and choroid plexus progressively increased and eventually exceeded the blood concentrations of ENT-03, the compound appears to be eliminated from the brain at a slower rate than from the circulation. The persistence of ENT-03 within the brain might explain the extended pharmacodynamic effect observed following a single intracerebroventricular injection. The accumulation of ENT-03 within the choroid plexus and its presence in the CSF suggests that ENT-03 could access all brain tissues bathed by the CSF, including the ependymal lining of the ventricles.

Since ENT-03 inhibits PTP1B, we investigated whether levels of phosphorylated proteins known to be substrates for this regulatory

phosphatase were increased following administration of the compound. In particular, both the PI3K-AKT and JAK-STAT3 pathways, engaged by the insulin and leptin receptors, are regulated by PTP1B[17] and are known to function within the arcuate nucleus in the regulation of food intake and adiposity. Indeed, mice fed ad libitum with laboratory chow, treated for 2 weeks with ENT-03 (i.p., 2 mg/kg, twice weekly) displayed robust immune-staining of pSTAT3 within the arcuate nucleus, lateral to the heavily stained NPY-rich zone in contact with the third ventricle (Figure 7). Although the increased pSTAT3 signal falls within the region containing leptin receptor-expressing neurons, STAT3 is also activated by numerous cytokines, such as tumour necrosis factor-α and ciliary neurotrophic factor,[19] both of which can suppress food intake. The specific intracellular pathways impacted by ENT-03 remain to be determined.

We also observed intense pSTAT3 immuno-staining of the ependymal lining of the third ventricle above the arcuate nucleus. The pSTAT3-positive cells were located immediately beneath the ependymal layer, within the subventricular zone, in the position occupied by tanycytes that play metabolic and neurogenic roles. The specific cell types within the subventricular zone that ENT-03 targets remain to be identified.

It should be understood that our data support, but do not confirm, that the metabolic effects of ENT-03 result from inhibition of PTP1B activity within the brain. In further support of this hypothesis, mice in which neuronal (but not liver or muscle) PTP1B has been knocked out substantially recapitulate the phenotype of whole-body PTP1B knockout and do not develop insulin resistance nor obesity on a high-fat diet,[28] similar to observations with ENT-03 administration. In addition, an analogue of trodusquemine (MSI-1521) that lacks the sulphate moiety on C-24, has lost both PTP1B inhibitory activity (Zasloff, unpublished) and effects on food intake, body weight and metabolic parameters in mice.[2]

Which neuronal circuits are activated following arrival of ENT-03 within the arcuate nucleus? Since the arcuate nucleus, central to energy homeostasis, sends projections throughout the subcortical brain and brainstem we addressed this question by conducting a whole-brain study capable of both resolving the cFos transcriptional activity of individual neuronal cells and precisely mapping them to specific anatomical locations. ENT-03 administration activated over 40 distinct anatomical sites. The principal areas activated lie within the hypothalamus and brainstem. Signals from various hypothalamic nuclei converge on the PVH, engaging neurons that control autonomic output. Distinct neuronal populations within the PVH influence energy homeostasis, suppressing feeding behaviour, increasing energy expenditure, or both.[29] Polysynaptic pathways relay these directives to the periphery via the nucleus tractus solitarius, and dorsal motor nucleus of the vagus, along cholinergic efferent vagal pathways.[30] Cholinergic activation increases hepatic glucose uptake, glycogenesis[31] and lipolysis.[32,33] Sympathetic signals originating in the PVH project to the intermediolateral nucleus of the spinal cord and are carried via adrenergic nerves to the liver.[33] Sympathetic stimulation increases hepatic glycogenolysis, glucose output and lipogenesis.[33] By balancing signals from both limbs of the autonomic pathway, the PVH can thus modulate pancreatic secretion,[34] adipose lipid storage,[32] thermogenesis by brown adipose tissue,[35] peripheral glucose uptake,[36] and lipolytic activity in the liver.[32]

Dysregulation of the hypothalamic–hepatic autonomic axis is emerging as an important factor in the pathology of aging,[37] metabolic syndrome and obesity.[38] These conditions are associated with centrally mediated autonomic imbalance, characterized by increased indices of sympathetic activity and cholinergic underactivity.[39,40] High-fat diets stimulate hepatic sympathetic activity and increase hepatic lipid burden, whereas surgical or pharmacological ablation of hepatic sympathetic supply ameliorates steatosis.[41] Conversely, parasympathetic activation decreases hepatic lipid content and hepatic vagotomy worsens diet-induced steatohepatitis[42] and induces insulin resistance.[43]

In conclusion, ENT-03 acutely corrects hyperglycaemia in diabetic obese mice independently of weight loss. While ENT-03 causes animals to eat less and subsequently lose weight, endogenous energy stores are depleted to a greater extent than can be accounted for by the reduced food intake. ENT-03 shifts the dependence on exogenous sources to endogenous stores. The multiplicity of brain regions activated by ENT-03 reflects the complexity of signalling that must be integrated to achieve energy homeostasis. The effects of ENT-03 in individuals with obesity type 2 diabetes are currently being evaluated in phase 1 clinical trials.

AUTHOR CONTRIBUTIONS

CONFLICT OF INTEREST STATEMENT

Denise Barbut, William A. Kinney and M. Zasloff have equity in Enterin, Inc.

PEER REVIEW

The peer review history for this article is available at https://www.webofscience.com/api/gateway/wos/peer-review/10.1111/dom.15940.

DATA AVAILABILITY STATEMENT

The data that support the findings of this study are available from the corresponding author upon reasonable request.

ORCID

Michael Zasloff https://orcid.org/0000-0002-1453-9328

REFERENCES

1. Rao MN, Shinnar AE, Noecker LA, et al. Aminosterols from the dogfish shark Squalus acanthias. *J Nat Prod*. 2000;63:631-635.
2. Zasloff M, Williams JI, Chen Q, et al. A spermine-coupled cholesterol metabolite from the shark with potent appetite suppressant and anti-diabetic properties. *Int J Obes Relat Metab Disord*. 2001;25:689-697.
3. Ahima RS, Patel HR, Takahashi N, Qi Y, Hileman SM, Zasloff MA. Appetite suppression and weight reduction by a centrally active aminosterol. *Diabetes*. 2002;51:2099-2104.
4. Takahashi N, Qi Y, Patel HR, Ahima RS. A novel aminosterol reverses diabetes and fatty liver disease in obese mice. *J Hepatol*. 2004;41:391-398.
5. Krishnan N, Koveal D, Miller DH, et al. Targeting the disordered C terminus of PTP1B with an allosteric inhibitor. *Nat Chem Biol*. 2014;10:558-566.
6. Pandey NR, Zhou X, Zaman T, et al. LMO4 is required to maintain hypothalamic insulin signaling. *Biochem Biophys Res Commun*. 2014;450:666-672.
7. Lantz KA, Hart SGE, Planey SL, et al. Inhibition of PTP1B by trodus-quemine (MSI-1436) causes fat-specific weight loss in diet-induced obese mice. *Obesity (Silver Spring)*. 2010;18:1516-1523.
8. Smith AM, Maguire-Nguyen KK, Rando TA, Zasloff MA, Strange KB, Yin VP. The protein tyrosine phosphatase 1B inhibitor MSI-1436 stimulates regeneration of heart and multiple other tissues. *NPJ Regen Med*. 2017;2:4.
9. Ellis J. *Multiple Doses of Trodusquemine Improve Glucose Tolerance in Type 2 Diabetic Subjects*. 2071-PO (Abs), 69th. Scientific Sessions American Diabetes Association; 2009.
10. Hofmann AF, Hagey LR, Krasowski MD. Bile salts of vertebrates: structural variation and possible evolutionary significance. *J Lipid Res*. 2010;51:226-246.
11. Ogundare M, Theofilopoulos S, Lockhart A, et al. Cerebrospinal fluid steroidomics: are bioactive bile acids present in brain? *J Biol Chem*. 2010;285:4666-4679.
12. Crick PJ, Beckers L, Baes M, van Veldhoven PP, Wang Y, Griffiths WJ. The oxysterol and cholestenoic acid profile of mouse cerebrospinal fluid. *Steroids*. 2015;99:172-177.
13. Meaney S, Heverin M, Panzenboeck U, et al. Novel route for elimination of brain oxysterols across the blood-brain barrier: conversion into 7alpha-hydroxy-3-oxo-4-cholestenoic acid. *J Lipid Res*. 2007;48:944-951.
14. Kinney WA, Phillip Cox D, Jones SR, et al. Asymmetric synthesis of ENT-03, the predicted mammalian ortholog of the dog fish shark aminosterol trodusquemine (MSI-1436). *Tetrahedron Lett*. 2024;148:155220. https://doi.org/10.1016/j.tetlet.2024.155220
15. Luque RM, Kineman RD. Impact of obesity on the growth hormone axis: evidence for a direct inhibitory effect of hyperinsulinemia on pituitary function. *Endocrinology*. 2006;147:2754-2763.
16. Larson BA, Sinha YN, Vanderlaan WP. Serum growth hormone and prolactin during and after the development of the obese-hyperglycemic syndrome in mice. *Endocrinology*. 1976;98:139-145.
17. Feldhammer M, Uetani N, Miranda-Saavedra D, Tremblay ML. PTP1B: a simple enzyme for a complex world. *Crit Rev Biochem Mol Biol*. 2013;48:430-445.
18. Seely BL, Staubs PA, Reichart DR, et al. Protein tyrosine phosphatase 1B interacts with the activated insulin receptor. *Diabetes*. 1996;45:1379-1385.
19. Venema W, Severi I, Perugini J, et al. Ciliary neurotrophic factor acts on distinctive hypothalamic arcuate neurons and promotes leptin entry into and action on the mouse hypothalamus. *Front Cell Neurosci*. 2020;14:140.
20. Ladyman SR, Grattan DR. JAK-STAT and feeding. *JAKSTAT*. 2013;2:e23675.
21. Hansen HH, Perens J, Roostalu U, et al. Whole-brain activation signatures of weight-lowering drugs. *Mol Metab*. 2021;47:101171.
22. Barbut D, Baur J, Titchenell P, et al. ENT-03, a centrally acting endogenous Spermine bile acid with PTP1B inhibitory activity has potent effects on metabolism and weight in a mouse model of diet induced obesity (DIO). *Diabetes*. 2023;72:854.
23. Pucci A, Batterham RL. Mechanisms underlying the weight loss effects of RYGB and SG: similar, yet different. *J Endocrinol Invest*. 2019;42:117-128.
24. Flynn CR, Albaugh VL, Cai S, et al. Bile diversion to the distal small intestine has comparable metabolic benefits to bariatric surgery. *Nat Commun*. 2015;6:7715.
25. van Dijk G, Evers SS, Guidotti S, Thornton SN, Scheurink AJW, Nyakas C. The lateral hypothalamus: a site for integration of nutrient and fluid balance. *Behav Brain Res*. 2011;221:481-487.
26. Koch C, Augustine RA, Steger J, et al. Leptin rapidly improves glucose homeostasis in obese mice by increasing hypothalamic insulin sensitivity. *J Neurosci*. 2010;30:16180-16187.
27. German J, Kim F, Schwartz GJ, et al. Hypothalamic leptin signaling regulates hepatic insulin sensitivity via a neurocircuit involving the vagus nerve. *Endocrinology*. 2009;150:4502-4511.
28. Bence KK, Delibegovic M, Xue B, et al. Neuronal PTP1B regulates body weight, adiposity and leptin action. *Nat Med*. 2006;12:917-924.
29. Sutton AK, Myers MG Jr, Olson DP. The role of PVH circuits in leptin action and energy balance. *Annu Rev Physiol*. 2016;78:207-221.
30. Berthoud HR. The vagus nerve, food intake and obesity. *Regul Pept*. 2008;149:15-25.
31. Shimazu T, Matsushita H, Ishikawa K. Cholinergic stimulation of the rat hypothalamus: effects of liver glycogen synthesis. *Science*. 1976;194:535-536.
32. Stanley S, Pinto S, Segal J, et al. Identification of neuronal subpopulations that project from hypothalamus to both liver and adipose tissue polysynaptically. *Proc Natl Acad Sci U S A*. 2010;107:7024-7029.
33. Amir M, Yu M, He P, Srinivasan S. Hepatic autonomic nervous system and neurotrophic factors regulate the pathogenesis and progression of non-alcoholic fatty liver disease. *Front Med (Lausanne)*. 2020;7:62.
34. Jansen AS, Hoffman JL, Loewy AD. CNS sites involved in sympathetic and parasympathetic control of the pancreas: a viral tracing study. *Brain Res*. 1997;766:29-38.
35. Song CK, Vaughan CH, Keen-Rinehart E, Harris RBS, Richard D, Bartness TJ. Melanocortin-4 receptor mRNA expressed in sympathetic outflow neurons to brown adipose tissue: neuroanatomical and functional evidence. *Am J Physiol Regul Integr Comp Physiol*. 2008;295:R417-R428.
36. Marino JS, Xu Y, Hill JW. Central insulin and leptin-mediated autonomic control of glucose homeostasis. *Trends Endocrinol Metab*. 2011;22:275-285.
37. Zhang G, Li J, Purkayastha S, et al. Hypothalamic programming of systemic ageing involving IKK-beta NF-kappaB and GnRH. *Nature*. 2013;497:211-216.
38. Scherer T, Sakamoto K, Buettner C. Brain insulin signalling in metabolic homeostasis and disease. *Nat Rev Endocrinol*. 2021;17:468-483.

39. Lambert GW, Straznicky NE, Lambert EA, Dixon JB, Schlaich MP. Sympathetic nervous activation in obesity and the metabolic syndrome—causes, consequences and therapeutic implications. *Pharmacol Ther*. 2010;126:159-172.

40. Schlaich M, Straznicky N, Lambert E, Lambert G. Metabolic syndrome: a sympathetic disease? *Lancet Diabetes Endocrinol*. 2015;3:148-157.

41. Hurr C, Simonyan H, Morgan DA, Rahmouni K, Young CN. Liver sympathetic denervation reverses obesity-induced hepatic steatosis. *J Physiol*. 2019;597:4565-4580.

42. Nishio T, Taura K, Iwaisako K, et al. Hepatic vagus nerve regulates Kupffer cell activation via alpha7 nicotinic acetylcholine receptor in nonalcoholic steatohepatitis. *J Gastroenterol*. 2017;52:965-976.

43. Latour MG, Lautt WW. The hepatic vagus nerve in the control of insulin sensitivity in the rat. *Auton Neurosci*. 2002;95:125-130.

SUPPORTING INFORMATION

Additional supporting information can be found online in the Supporting Information section at the end of this article.

How to cite this article: Barbut D, Kinney WA, Chen H-H, et al. A novel, centrally acting mammalian aminosterol, ENT-03, induces weight loss in obese and lean rodents. *Diabetes Obes Metab*. 2024;1-12. doi:10.1111/dom.15940